



the
abdus salam
international
centre
for theoretical
physics



XA0304364



**HIGH ELECTRON THERMAL CONDUCTIVITY
OF CHIRAL CARBON NANOTUBES**

S.Y. Mensah

F.K.A. Allotey

George Nkrumah

and

N.G. Mensah

preprint

United Nations Educational Scientific and Cultural Organization
and
International Atomic Energy Agency
THE ABDUS SALAM INTERNATIONAL CENTRE FOR THEORETICAL PHYSICS

**HIGH ELECTRON THERMAL CONDUCTIVITY
OF CHIRAL CARBON NANOTUBES**

S.Y. Mensah

*Department of Physics, Laser and Fibre Optics Centre, University of Cape Coast,
Cape Coast, Ghana*

and

The Abdus Salam International Centre for Theoretical Physics, Trieste, Italy,

F.K.A. Allotey

Institute of Mathematical Sciences, Accra, Ghana

and

The Abdus Salam International Centre for Theoretical Physics, Trieste, Italy,

George Nkrumah

Department of Physics, University of Ghana, Legon, Accra, Ghana

and

N.G. Mensah

*Department of Mathematics, University of Cape Coast,
Cape Coast, Ghana.*

MIRAMARE – TRIESTE

November 2003

Abstract

Solving the Boltzmann kinetic equation with energy dispersion relation obtained in the tight-binding approximation, the carrier thermal conductivity κ_e of a chiral carbon nanotube (CCNT) was determined. The dependence of κ_e on temperature T , chiral geometric angle ϕ_h and overlap integrals Δ_z and Δ_s were obtained. The results were numerically analysed. Unusually high values of κ_e were observed suggesting that κ_e is nontrivial in the calculation of the thermal conductivity κ of CCNT. More interestingly we noted also that at 104 K and for Δ_z and Δ_s values of 0.020 eV and 0.0150 eV respectively the κ_e value is about 41000 W/mK as reported for a 99.9% pure ^{12}C crystal. We predict that the electron thermal conductivity of CCNT should exceed 200,000 W/mK at ~ 80 K.

1 Introduction

Due to the numerous applications of carbon nanotubes (CNTs), there has been several publications on this novel material. The past decade witnessed significant research efforts in efficient and high-yield nanotube growth methods. The result of which has led to a wide availability of nanotube materials. CNTs are highly unusual electrical conductors, the strongest known fibres and excellent thermal conductors. Many potentially important applications have been explored, including the use of nanotubes as nanoprobe tips [1], fields emitters [2]-[6] (CNTs might soon be used as field emitters in flat-screen televisions), storage of filtering media [7] and nanoscale electronic devices [8]-[19].

Carbon nanotubes, the carbon atoms of which are held together by strong sp^2 and sp^3 bonds consist of seamless graphitic cylinders a few nanometers in diameter and closed at either ends with caps containing pentagonal rings of carbon atoms. CNTs can manifest either metallic or semiconductor properties, depending on its cross-sectional radius and geometric chiral angle [20]-[22].

It is known that, as the dimensions of electronic and mechanical devices are shrunk into nanometer dimensions, the thermal conductivity becomes quite important since functioning electronic, piezoelectric, and thermogalvanic devices may require that significant energy be dissipated in a small region [23]. Consequently, it is of interest to develop reliable theoretical and computational methods for predicting the thermal properties of nanoscale materials and devices.

There are two major approaches to theoretical studies of thermal conductivities of materials

- (1) The most fundamental approach is to base the calculations on the first principle atomistic simulations, i.e. using the Green-Kubo relation derived from linear response theory to extract the thermal conductivity from the energy current correlation functions. Both equilibrium and nonequilibrium dynamic simulations [24]-[26] have been reported for various systems. Combination of equilibrium and nonequilibrium molecular dynamics simulations with accurate carbon potentials have been used to determine the thermal conductivity of carbon nanotubes and its dependence on temperature [27].
- (2) It can also be studied using continuum models and kinetic theories such as the Boltzmann transport equation. For example, Walkauskas et al. [28] calculated the lattice thermal conductivity of GaAs wires; Balandin and Weng [29] calculated the thermal conductivity reduction in the Si quantum well. The advantage of using Boltzmann equation (BE) is that large systems can be studied reasonably quickly. In addition, solving the integro-differential BE for general cases is nontrivial.

One can generally partition the thermal conductivity of material into the charge carrier (i.e. electron or hole) component κ_e which depends on the electronic band structure, electron scattering and electron-phonon interaction, and the lattice (or phonon) component κ_L which

depends mainly on phonon and phonon scattering. In dielectrics, $\kappa_L \gg \kappa_e$, while in metals $\kappa_e \gg \kappa_L$. In semiconductors the value of κ_e is strongly dependent on the composition of the semiconductor, and the value κ_L is generally greater than the value of κ_e .

Research shows that CNTs are expected to have high thermal conductivity [27, 30, 31]. Experiments have confirmed unusually high thermal conductivity in CNTs [32, 33] and indicated that thermal conductivity of single walled carbon nanotubes is dominated by phonons at all temperatures. Moreover the high value of thermal conductivity obtained in an isolated (10,10) CNT at room temperature by Berber et al. [27] was associated with the long mean free path of phonons.

In this paper, we calculate electron thermal conductivity of single-walled chiral carbon nanotube (SWNTs) using Boltzmann kinetic equation and a model based on infinitely long carbon atoms wrapped along a base helix of (SWNTs) [34, 35]. We noted an unusually high value of electron thermal conductivity similar to that obtained by Berber et al. for the lattice thermal conductivity. This indicates that the contribution of κ_e is nontrivial in calculating the thermal conductivity of (SWNTs). We also want to state that the model used is good as is also confirmed by [34, 35], where it is stated that the model is good for doped CNTs. We further observed that κ_e strongly depends on the geometric chiral angle ϕ_h , temperature T , the real overlapping integrals for jumps along the tubular axis Δ_z and the base helix Δ_s . It is worth noting that varying these parameters can give rise to unusually high electron thermal conductivity. This in our opinion suggests the use of (CNTs) as efficient thermal conductance.

This paper is organised as follows: in section 2 we establish the theory and solution of the problem, and in section 3 we discuss the results and draw conclusions.

2 Theory and Results

Single walled-carbon nanotube (SWNT) is considered as an infinitely long chain of carbon atoms wrapped along a base helix. The problem is considered in the semiclassical approximation, starting with the Boltzmann kinetic equation [36],

$$\frac{\partial f(r, p, t)}{\partial t} + v(p) \frac{\partial f(r, p, t)}{\partial r} + eE \frac{\partial f(r, p, t)}{\partial p} = - \frac{f(r, p, t) - f_0(p)}{\tau} \quad (1)$$

Here $f(r, p, t)$ is the distribution function, $f_0(p)$ is the equilibrium distribution function, $v(p)$ is the electron velocity, E is a weak constant applied field, r is the electron position, p is the electron dynamical momentum, τ is the relaxation time and e is the electron charge. The collision integral is taken in the τ approximation and further assumed constant. Eq. (1) is solved by perturbation approach treating the second term as the perturbation. In the linear approximation of ∇T and $\nabla \mu$, μ is the chemical potential, we obtain

$$\begin{aligned}
f(p) &= \tau^{-1} \int_0^\infty \exp\left(-\frac{t}{\tau}\right) f_0(p - eEt) dt + \int_0^\infty \exp\left(-\frac{t}{\tau}\right) dt \\
&\quad \times \left([\varepsilon(p - eEt) - \mu] \frac{\nabla T}{T} + \nabla \mu \right) v(p - eEt) \frac{\partial f_0(p - eEt)}{\partial \varepsilon}
\end{aligned} \tag{2}$$

here $\varepsilon(p)$ is the electron energy.

The thermal current density \mathbf{q} is given as

$$\mathbf{q} = \sum_p [\varepsilon(p) - \mu] \mathbf{v}(p) f(p) \tag{3}$$

Substituting Eq(2) into Eq(3) and making the transformation

$$p - eEt \rightarrow p$$

we obtain for the thermal current density

$$\begin{aligned}
\mathbf{q} &= \tau^{-1} \int_0^\infty \exp\left(-\frac{t}{\tau}\right) dt \sum_p [\varepsilon(p - eEt) - \mu] \mathbf{v}(p - eEt) f_0(p) \\
&\quad + \int_0^\infty \exp\left(-\frac{t}{\tau}\right) dt \sum_p [\varepsilon(p - eEt) - \mu] \left\{ [\varepsilon(p) - \mu] \frac{\nabla T}{T} + \nabla \mu \right\} \\
&\quad \times \left\{ v(p) \frac{\partial f_0(p)}{\partial \varepsilon} \right\} \mathbf{v}(p - eEt)
\end{aligned} \tag{4}$$

We resolve the thermal current density along the tubular axis (z axis) and the base helix respectively, neglecting the interference between the axial and the helical paths connecting a pair of atoms, so that transverse motion quantization is ignored. Then using the following transformation:

$$\sum_p \rightarrow \frac{2}{(2\pi\hbar)^2} \int_{-\frac{\pi}{d_s}}^{\frac{\pi}{d_s}} dp_s \int_{-\frac{\pi}{d_z}}^{\frac{\pi}{d_z}} dp_z$$

we obtain

$$\begin{aligned}
Z' &= \frac{2\tau^{-1}}{(2\pi\hbar)^2} \int_0^\infty \exp\left(-\frac{t}{\tau}\right) dt \int_{-\frac{\pi}{d_s}}^{\frac{\pi}{d_s}} dp_s \int_{-\frac{\pi}{d_z}}^{\frac{\pi}{d_z}} dp_z [\varepsilon(p - eEt) - \mu] v_z(p - eEt) f_0(p) \\
&\quad + \frac{2}{(2\pi\hbar)^2} \int_0^\infty \exp\left(-\frac{t}{\tau}\right) dt \int_{-\frac{\pi}{d_s}}^{\frac{\pi}{d_s}} dp_s \int_{-\frac{\pi}{d_z}}^{\frac{\pi}{d_z}} dp_z [\varepsilon(p - eEt) - \mu] \\
&\quad \times \left\{ [\varepsilon(p) - \mu] \frac{\nabla_z T}{T} + \nabla_z \mu \right\} \left\{ v_z(p) \frac{\partial f_0(p)}{\partial \varepsilon} \right\} v_z(p - eEt)
\end{aligned} \tag{5}$$

and

$$\begin{aligned}
S' &= \frac{2\tau^{-1}}{(2\pi\hbar)^2} \int_0^\infty \exp\left(-\frac{t}{\tau}\right) dt \int_{-\frac{\pi}{d_s}}^{\frac{\pi}{d_s}} dp_s \int_{-\frac{\pi}{d_z}}^{\frac{\pi}{d_z}} dp_z [\varepsilon(p - eEt) - \mu] v_s(p - eEt) f_0(p) \\
&\quad + \frac{2}{(2\pi\hbar)^2} \int_0^\infty \exp\left(-\frac{t}{\tau}\right) dt \int_{-\frac{\pi}{d_s}}^{\frac{\pi}{d_s}} dp_s \int_{-\frac{\pi}{d_z}}^{\frac{\pi}{d_z}} dp_z [\varepsilon(p - eEt) - \mu] \\
&\quad \times \left\{ [\varepsilon(p) - \mu] \frac{\nabla_s T}{T} + \nabla_s \mu \right\} \left\{ v_s(p) \frac{\partial f_0(p)}{\partial \varepsilon} \right\} v_s(p - eEt)
\end{aligned} \tag{6}$$

where Z' and S' are the thermal current along the tubular axis and the base helix respectively. The integrations are carried out over the first Brillouin zone. From these two components, the axial and circumferential thermal current density is given respectively as

$$q_z = Z' + S' \sin \theta_h \quad q_c = S' \cos \theta_h \quad (7)$$

where θ_h is the geometric chiral angle (GCA).

The energy $\varepsilon(p)$ of the electrons, calculated using the tight binding approximation is given as expressed in [34] as follows:

$$\varepsilon(p) = \varepsilon_o - \Delta_s \cos \frac{p_s d_s}{\hbar} - \Delta_z \cos \frac{p_z d_z}{\hbar} \quad (8)$$

ε_o is the energy of an outer-shell electron in an isolated carbon atom, Δ_s and Δ_z are the real overlapping integrals for jumps along the respective coordinates, p_s and p_z are the carrier momentum along the base helix and the tubular axis respectively, \hbar is $h/2\pi$ and h is Planck's constant. d_s is the distance between the site n and $n + 1$ along the base helix and d_z is the distance between the site n and $n + N$ along the tubular axis.

For a non-degenerate electron gas, we use the Boltzmann equilibrium distribution function $f_0(p)$ as expressed in [37], i.e.,

$$f_0(p) = C \exp \left(\frac{\Delta_s \cos \frac{p_s d_s}{\hbar} + \Delta_z \cos \frac{p_z d_z}{\hbar} + \mu - \varepsilon_o}{kT} \right) \quad (9)$$

where C is determined by the condition

$$C = \frac{d_s d_z n_o}{2 \exp \left(\frac{\mu - \varepsilon_o}{kT} \right) I_0(\Delta_s^*) I_0(\Delta_z^*)}$$

and n_o is charge density, $I_n(x)$ is the modified Bessel function of order n and k is Boltzmann's constant.

The components v_s and v_z of the electron velocity \mathbf{v} are given by

$$v_s(p_s) = \frac{\partial \varepsilon(p)}{\partial p_s} = \frac{\Delta_s d_s}{\hbar} \sin \frac{p_s d_s}{\hbar} \quad (10)$$

and

$$v_z(p_z) = \frac{\partial \varepsilon(p)}{\partial p_z} = \frac{\Delta_z d_z}{\hbar} \sin \frac{p_z d_z}{\hbar} \quad (11)$$

Using Eqs. (5)–(11) and the fact that $E_s = E_z \sin \theta_h$, $\nabla_s T = \nabla_z T \sin \theta_h$, and $E = -\nabla \phi$, we obtain the circumferential q_c and axial q_z thermal current densities after a cumbersome calculation as follows,

$$\begin{aligned} q_c &= \sigma_s \frac{kT}{e} \sin \theta_h \cos \theta_h \{ \xi - \Delta_s^* B_s - \Delta_z^* A_z \} \nabla_z \left(\frac{\mu}{e} - \phi \right) \\ &+ \sigma_s \frac{k^2 T}{e^2} \sin \theta_h \cos \theta_h \left\{ \xi^2 - 2\Delta_s^* \xi B_s - 2\Delta_z^* \xi A_z + (\Delta_s^*)^2 C_s \right. \\ &\left. + 2\Delta_s^* \Delta_z^* B_s A_z + (\Delta_z^*)^2 \left(1 - \frac{A_z}{\Delta_z^*} \right) \right\} \nabla_z T \end{aligned} \quad (12)$$

$$\begin{aligned}
q_z &= \sigma_z \frac{kT}{e} \left\{ \xi - \Delta_z^* B_z - \Delta_s^* A_s + \sin^2 \theta_h (\xi - \Delta_s^* B_s - \Delta_z^* A_z) \right\} \nabla_z \left(\frac{\mu}{e} - \phi \right) \\
&+ \frac{k^2 T}{e^2} \left\{ \sigma_z \left[\xi^2 - 2\Delta_z^* \xi B_z - 2\Delta_s^* \xi A_s + (\Delta_z^*)^2 C_z \right. \right. \\
&+ 2\Delta_z^* \Delta_s^* B_z A_s + (\Delta_s^*)^2 \left(1 - \frac{A_s}{\Delta_s^*} \right) \left. \right] + \sigma_s \sin^2 \theta_h \left[\xi^2 - 2\Delta_s^* \xi B_s \right. \\
&\left. \left. - 2\Delta_z^* \xi A_z + (\Delta_s^*)^2 C_s + 2\Delta_s^* \Delta_z^* B_s A_z + (\Delta_z^*)^2 \left(1 - \frac{A_z}{\Delta_z^*} \right) \right] \right\} \nabla_z T \quad (13)
\end{aligned}$$

Here

$$\begin{aligned}
\xi &= \frac{\varepsilon_0 - \mu}{kT} \quad A_i = \frac{I_1(\Delta_i^*)}{I_0(\Delta_i^*)}, \quad B_i = \frac{I_0(\Delta_i^*)}{I_1(\Delta_i^*)} - \frac{2}{\Delta_i^*} \\
C_i &= 1 - \frac{3}{\Delta_i^*} \frac{I_0(\Delta_i^*)}{I_1(\Delta_i^*)} + \frac{6}{(\Delta_i^*)^2}, \\
\sigma_i &= \frac{n_o e^2 \Delta_i d_i^2 \tau}{\hbar^2} \frac{I_1(\Delta_i^*)}{I_0(\Delta_i^*)}, \quad \Delta_i^* = \frac{\Delta_i}{kT} \quad \text{where } i = s, z
\end{aligned}$$

Eqs. (12) and (13) are the results for weak electric field E . The coefficient of $\nabla_z T$ in Eqs. (12) and (13) defines the thermal conductivity. Of interest to us is the axial component of the thermal conductivity κ_z . From Eq. (13), κ_z is given by

$$\begin{aligned}
\kappa_z &= \frac{k^2 T}{e^2} \left\{ \sigma_z \left[\xi^2 - 2\Delta_z^* \xi B_z - 2\Delta_s^* \xi A_s + (\Delta_z^*)^2 C_z \right. \right. \\
&+ 2\Delta_z^* \Delta_s^* B_z A_s + (\Delta_s^*)^2 \left(1 - \frac{A_s}{\Delta_s^*} \right) \left. \right] + \sigma_s \sin^2 \theta_h \left[\xi^2 - 2\Delta_s^* \xi B_s \right. \\
&\left. \left. - 2\Delta_z^* \xi A_z + (\Delta_s^*)^2 C_s + 2\Delta_s^* \Delta_z^* B_s A_z + (\Delta_z^*)^2 \left(1 - \frac{A_z}{\Delta_z^*} \right) \right] \right\} \quad (14)
\end{aligned}$$

3 Results, Discussion and Conclusion

In this paper we analysed the electron thermal conductivity κ_e , given by Eq. (14), of a chiral CNT using the approach adopted in [37, 38]. It is noted that κ_e depends on temperature T chiral geometric angle ϕ_h and overlap integrals Δ_z and Δ_s . We further analysed the results by using numerical methods. We sketched the graphs of the dependence of κ_e on temperature T for various values of Δ_z and Δ_s . In Fig.1 for example, the graph is for $\Delta_s = 0.0156$ eV and $\Delta_z = 0.0204$ eV. In this figure our calculations suggested that at $T = 100$ K carbon nanotubes show an unusually high thermal conductivity value of about 37500 W/mK. This value lies very close to the highest value observed in any solid, $\kappa = 41000$ W/mK, that has been reported [39] for a 99.9% pure ^{12}C crystal at 104 K. Despite of the decrease of κ_e above 100 K the room temperature value of about 11000 W/mK is very high and is about 3 times the value reported for nearly isotopically pure diamond [39].

We want to emphasise that this result compares quite well with that of the lattice thermal conductivity κ_e of (10,10) CNT calculated by Berber et al. [27] see the insertion in figure one.

In Fig.2 we sketched κ_e against T for $\Delta_s = 0.0150$ eV and varied Δ_z from 0.010 eV to 0.048 eV. Very interestingly we noted that the peak values of κ_e shift towards the right from 100 K to 200 K after which κ_e become constant for the changing values of Δ_z . This is to be expected because thermal conductivity is proportional to the thermal capacity and according to Delong-Petit law the thermal capacity is constant. When $\Delta_z = 0.020$ eV the peak value of κ_e occurs at 104 K and is about 41000 W/mK as reported in [39] for a 99.9% pure 12 C crystal. Again the peak values increase with increase of Δ_z . At $\Delta_z = 0.048$ eV we observed a giant electron thermal conductivity at ~ 80 K of the value of about 200000 W/mK, which corresponds to a similar observation noted in [39] for 99.9% 12 C diamond crystal.

In Fig.3, we herein examine κ_e against T for $\Delta_z = 0.0159$ eV and varying values of Δ_s from 0.010 eV to 0.048 eV. We noted that the peak values of κ_e decrease with increasing value of Δ_s , and also κ_e assumes a constant value at high temperatures.

In conclusion, electron thermal conductivity of chiral CNT has been investigated theoretically. Unusually high values of κ_e is reported for varying values of Δ_z and Δ_s . Especially for Δ_z and Δ_s values of 0.0150 eV and 0.020 eV respectively and at 104 K the electron thermal conductivity is about 41000 W/mK. We predict giant thermal conductivity value of 200000 W/mK at about ~ 80 K.

Acknowledgements

This work was performed within the framework of the Associateship Scheme of the Abdus Salam International Centre for Theoretical Physics, Trieste, Italy. Financial support from the Swedish International Development Cooperation Agency is acknowledged.

References

- [1] H. Dai, E.W. Wong, C.M. Lieber, *Nature* (London) **384**, 147 (1996).
- [2] J.M. Bonard, J.P. Salvetat, T. Stockli and W.A. de Heer, *Appl. Phys. Lett.* **73** 918 (1998).
- [3] Q.H. Wang, T.D. Corrigan, T.Y. Dai and R.P.H. Chang, *Appl. Phys. Lett.* **70** 3308 (1997).
- [4] W.A. de Heer, A. Châtelain, D. Ugarte, *Science* **270**, 1179 (1995) *ibid* p. 1119.
- [5] A.G. Rinzler, J.H. Hafner, P. Nikolaev, L. Lou, S.G. Kim, D. Tománek, P. Nordlander, D.T. Colbert and R.E. Smalley, *Science* **269**, 1550 (1995).
- [6] V. Semet, Vu Thien Binh, P. Vincent, D. Guillot, K.B.K. Teo, M. Chhowalla, G.A.J. Amaratunga and W.I. Milne, *Appl. Phys. Lett.* **81**, 343 (2002).
- [7] A.C. Dillon, K.M. Jones, T.A. Bekkedahl, C.H. Kiang, D.S. Bethune and M.J. Heben, *Nature*, (London) **386**, 377 (1997).

- [8] L. Chico, V.H. Crespi, L.X. Benedict, S.G. Louie and M.L. Cohen, *Phys. Rev. Lett.* **76**, 971-974 (1996).
- [9] Ph. Lambin, A. Fonseca, J.P. Vigneron, J.B. Nagy and A.A. Lucas, *Chem. Phys. Lett.* **245**, 85-89 (1995).
- [10] R. Saito, G. Dresselhaus and M.S. Dresselhaus, *Phys. Rev. B* **53**, 2044-2050 (1996).
- [11] S.J. Tans, M.H. Devoret, H. Dai, A. Thess, R.E. Smalley, L.J. Geerligs and C. Dekker, *Nature (London)* **386**, 474 (1997).
- [12] M. Bockrath, D.H. Cobden, P.L. McEuen, N.G. Chopra, A. Zettl, A. Thess and R.E. Smalley, *Science* **275**, 1922 (1997).
- [13] R. Martel, T. Schmidt, H.R. Shea, T. Hertel and Ph. Avouris, *Appl. Phys. Lett.* **73**, 2447 (1998).
- [14] P.G. Collins, A. Zettl, H. Bando, A. Thess and R.E. Smalley, *Science* **278**, 5335 (1997).
- [15] Zhen Yao, H.W.C. Postma, L. Balents and C. Dekker, *Nature (London)* **402**, 273 (1999).
- [16] S.J. Tans, R.M. Verschueren and C. Dekker, *Nature* **393**, 49-52 (1998).
- [17] A. Bachtold, P. Hadley, T. Nakanishi and C. Dekker, *Science* **294**, 1317 (2001).
- [18] Y. Huang, et al., *Science*, **294**, 1313 (2001).
- [19] V. Derycke, R. Martel, J. Appenzeller and Ph. Avouris, *Nano Letters* **9**, 453 (2001).
- [20] J.W.G. Wildöer, L.C. Venema, A.G. Rinzler, R.E. Smalley and C. Dekker, *Nature (London)* **391**, 59 (1998).
- [21] T.W. Odom, J.L. Huang, P. Kim and C.M. Lieber, *Nature (London)* **391**, 62 (1998).
- [22] G.Ya. Slepyan, S.A. Maksimenko, A. Lakhtakia, O. Yevtushenko and A.V. Gusakov, *Phys. Rev. B* **60**, 17136 (1999).
- [23] Jianwei Che, Tahir Cagin, Weiqiao Deng and William A Goddard III, *J. Chemical Physics* **113**, 6888 (2000).
- [24] D.J. Evans, *Phys. Lett.* **91A**, 457 (1982).
- [25] D. Macgowan and D.J. Evans, *Phys. Lett.* **A117**, 414 (1986).
- [26] P.J. Davis and D.J. Evans, *J. Chem. Phys.* **103**, 4262 (1995).
- [27] S. Berber, Y.-K. Kwon and D. Tomànek, *Phys. Rev. Lett.* **84**, 4613 (2000).

- [28] S. Walkauskas, D. Broido, K. Kempa and T. Reineche, *J. Appl. Phys.* **85**, 2579 (1999).
- [29] A. Balandin and K. Wang, *Phys. Rev.* **B58**, 1544 (1998).
- [30] S. Iijima, *Nature (London)* **354**, 56 (1991).
- [31] M.S. Dresselhaus, G. Dresselhaus and P.C. Eklund, *Science of Fullerenes and Carbon Nanotubes* (Academic Press, San Diego, 1996).
- [32] J. Hone, M. Whitney, C. Piscoti and A. Zettl, *Phys. Rev. B* **59**, R2514 (1999).
- [33] J. Hone, M. Whitney and A. Zettl, *Synthetic Metals* **103**, 2498 (1999).
- [34] G.Ya Slepyan, S.A. Maksimenko, A. Lakhtakia, O.M. Yevtushenko and A.V. Gusakov, *Phys. Rev. B* **57**, 9485 (1988).
- [35] O.M. Yevtushenko, G.Ya Slepyan, S.A. Maksimenko, A. Lakhtakia and D.A. Ramanov, *Phys. Rev. Lett.* **79**, 1102 (1997).
- [36] S.Y. Mensah and G.K. Kangah, *J. Phys.: Condens Matter* **4**, 919 (1992).
- [37] S.Y. Mensah, F.K.A. Allotey, N.G. Mensah and G. Nkrumah, *J. Phys.: Condens. Matter* **13**, 5653 (2001).
- [38] S.Y. Mensah, F.K.A. Allotey, N.G. Mensah and G. Nkrumah, *Superlattices and Microstructures* **33**, 173 (2003).
- [39] Lanhua Wei, P. K. Kuo, R.L. Thomas, T. R. Anthony, and W. F. Banholzer, *Physical Rev. Lett.* **70** 3764(1993)

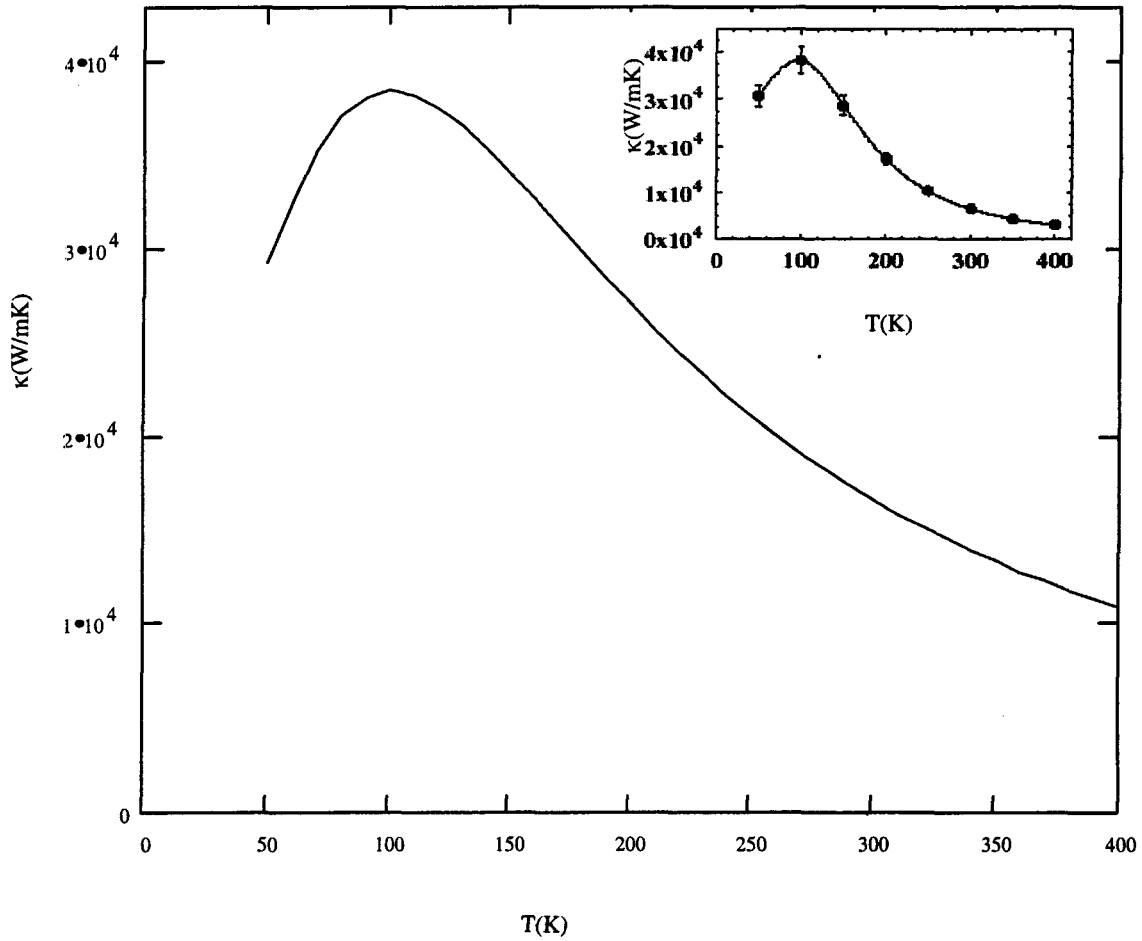


Figure1 The temperature dependence of the electron thermal conductivity for $\Delta_3=0.0156$ eV and $\Delta_2=0.0204$ eV
 The inserted is the graph obtained by Berber et al for lattice thermal conductivity of (10,10) CNT

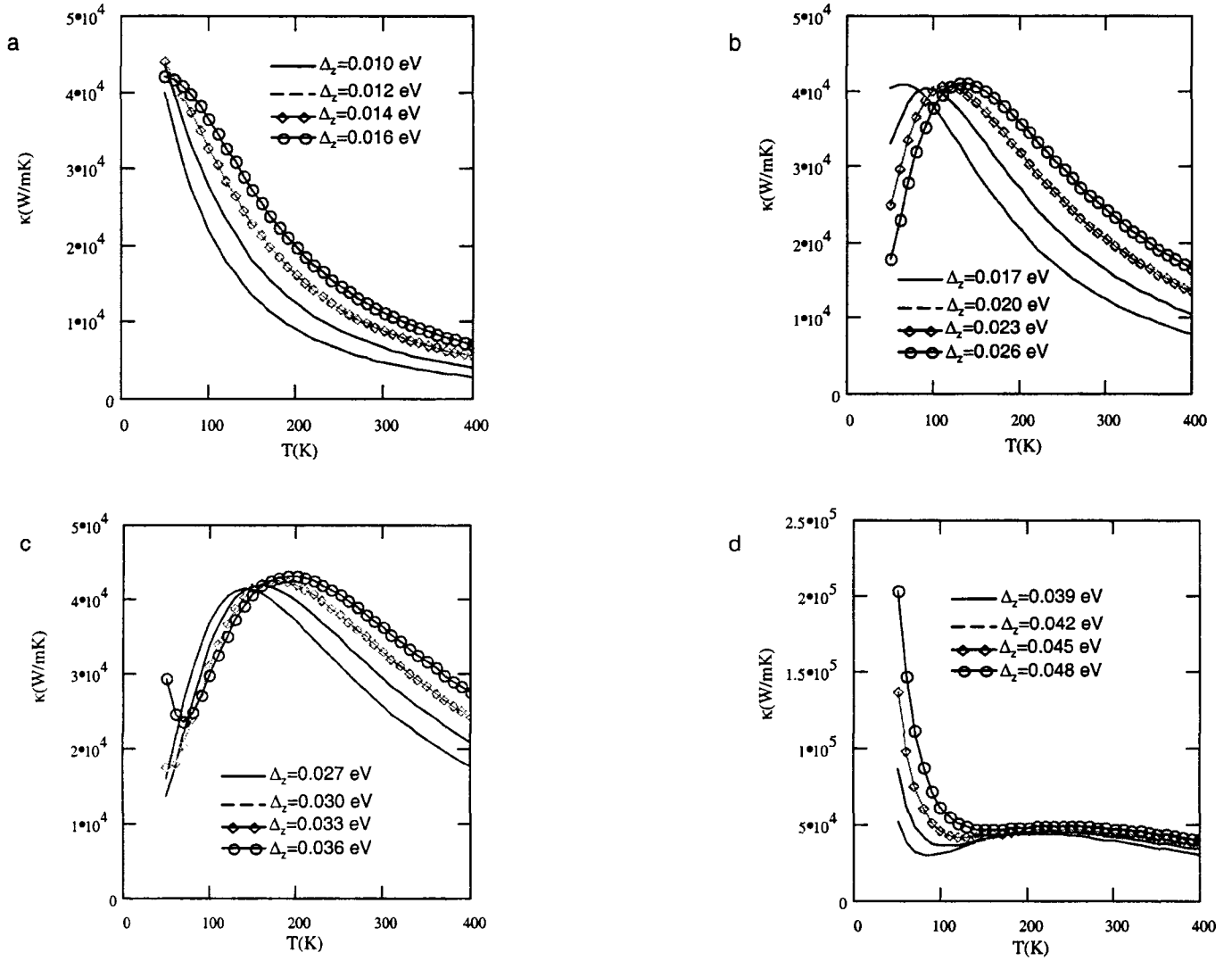


Figure 2 The temperature dependence of electron thermal conductivity for $\Delta_s=0.0150$ eV and Δ_z varied from 0.010 to 0.048 eV.

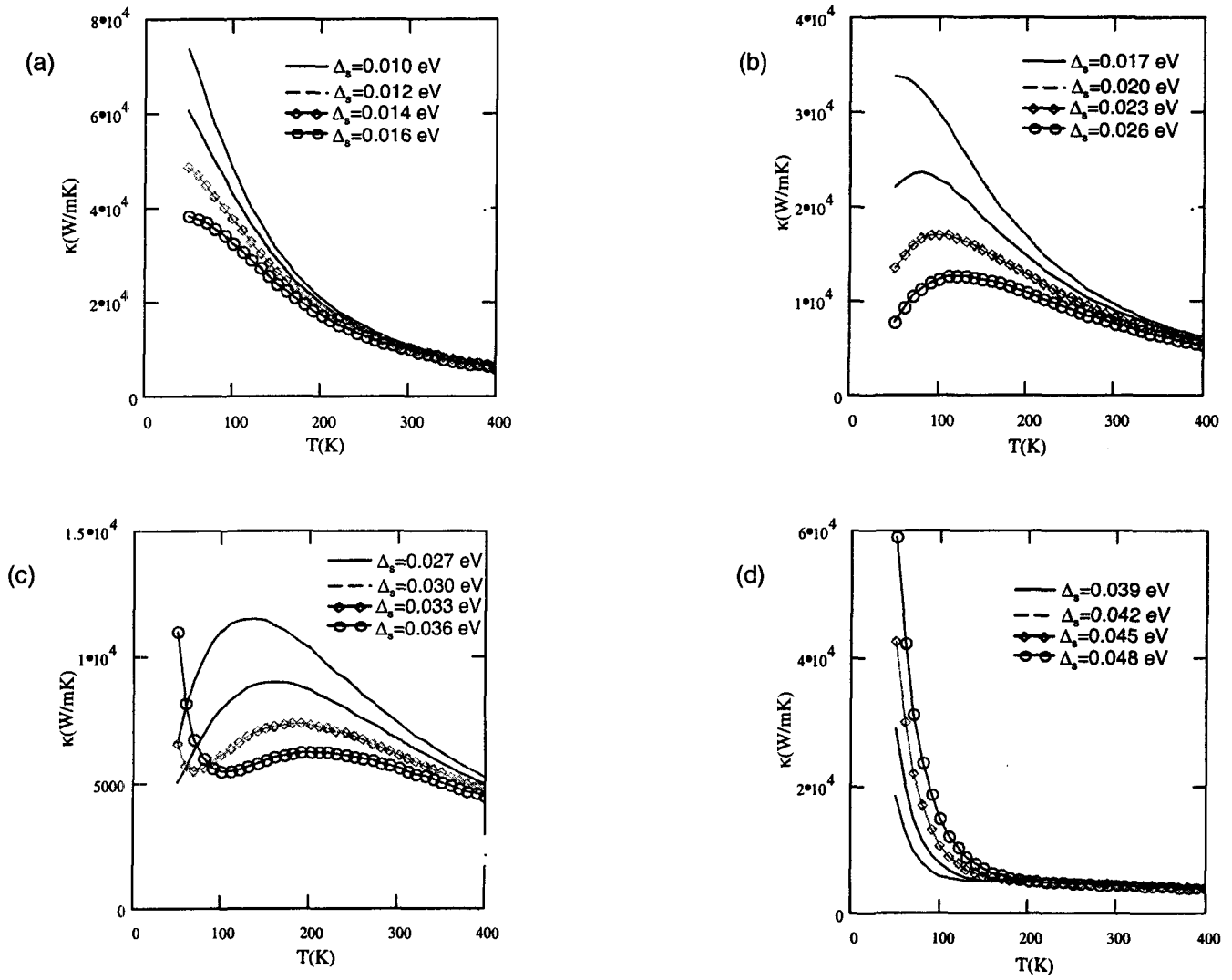


Figure 3 The temperature dependence of the electron thermal conductivity for $\Delta_z = 0.0150$ eV and Δ_s varied from 0.010 eV to 0.048 eV.